Journal of Chromatography A, 1225 (2012) 62–69

Contents lists available at SciVerse ScienceDirect

Journal of Chromatography A

journal homepage: www.elsevier.com/locate/chroma

Effects of resin ligand density on yield and impurity clearance in preparative cation exchange chromatography. I. Mechanistic evaluation

Jace Fogle*, Nina Mohan, Eric Cheung, Josefine Persson

Genentech Pharma Technical Development, 1 DNA Way MS 75A, South San Francisco, CA 94080, USA

ARTICLE INFO

Article history:
Received 15 July 2011
Received in revised form 2 November 2011
Accepted 15 December 2011
Available online 23 December 2011

Keywords:
Cation exchange chromatography
Monoclonal antibodies
Ligand density
High molecular weight variants
Charge variants
Aggregates
Host cell protein

ABSTRACT

The effects of resin ligand density on cation exchange chromatography performance in preparative monoclonal antibody purification processes were evaluated. A set of agarose-based cation exchange resins spanning a relatively wide range of ligand densities was tested using three different monoclonal antibodies with unique impurity profiles. Experiments were performed in bind-and-elute mode using gradient elution at both intermediate protein loadings and near saturation capacity. Ligand density did not affect clearance of high molecular weight variants under any of the conditions tested; however, ligand density did affect resolution of a basic charge variant in one case and changed host cell protein clearance in another instance. In general, the results indicate that the relationships between ligand density, retention, and resolution are affected by both characteristic charge and protein surface charge distribution.

1. Introduction

Cation exchange chromatography is commonly used as a downstream polishing step in recombinant monoclonal antibody purification processes. Requirements for this unit operation can include removal of product-related impurites such as aggregates and non-product-related impurities such as host cell proteins (HCP) and leached Protein A [1–5]. While upstream affinity chromatography steps often remove non-product-related impurities to trace levels, preparative purification processes usually rely on the cation exchange step to remove aggregates and other high molecular weight (HMW) species to levels that are safe for human therapeutic applications [6]. Process developers are faced with the challenge of designing downstream processes that provide robust impurity clearance while maximizing product yield, minimizing raw material cost, controlling cycle time, and operating within plant constraints.

There are an increasing number of commercial cation exchange resins available for use in large scale purification processes. These resins span a wide range of physical characteristics such as particle size, pore size and geometry, ligand density, and base matrix chemistry [7,8]. While the diverse nature of these products offers opportunity to screen resins for improved performance in specific applications, the relationships between resin properties and performance are not well understood. In particular, the effects of ligand density on impurity clearance have not been studied in a systematic manner for large scale monoclonal antibody purification processes.

Ligand density has been shown to influence both protein retention and mass transfer characteristics in ion exchange chromatography. Wu and Walters observed a switch in the elution order of lysozyme and cytochrome c on a set of five silica-based cation exchange resins with different ligand densities; cytochrome c eluted first on the lower ligand density resins, while lysozyme eluted first on the higher ligand density resins. They also noted pronounced band broadening at lower ligand densities which negatively impacted resolution of the two proteins [9]. Langford and co-workers used confocal microscopy techniques to show that resin ligand density can affect the ionic strength at which intraparticle transport switches from a pore diffusion to a homogenous diffusion mechanism [10]. Franke et al. found that ligand density affected resin porosity and the corresponding pore diffusivities [11]. These studies imply that the resolution of target protein and impurities could be significantly impacted by resin ligand density in preparative cation exchange processes; however, there is a lack of direct evidence to support this conclusion.

High molecular weight species such as protein aggregates can pose a particularly interesting challenge during process development because they may have similar tertiary structure and isoelectric point (pI) as the monomeric target protein [12]. Suda et al. showed that the characteristic charge of monomer and

* Corresponding author. Tel.: +1 650 467 4817; fax: +1 650 225 4049.
E-mail address: persson.josefine@gene.com (J. Fogle).

0021-9673/$ – see front matter © 2011 Elsevier B.V. All rights reserved.
doi:10.1016/j.chroma.2011.12.048

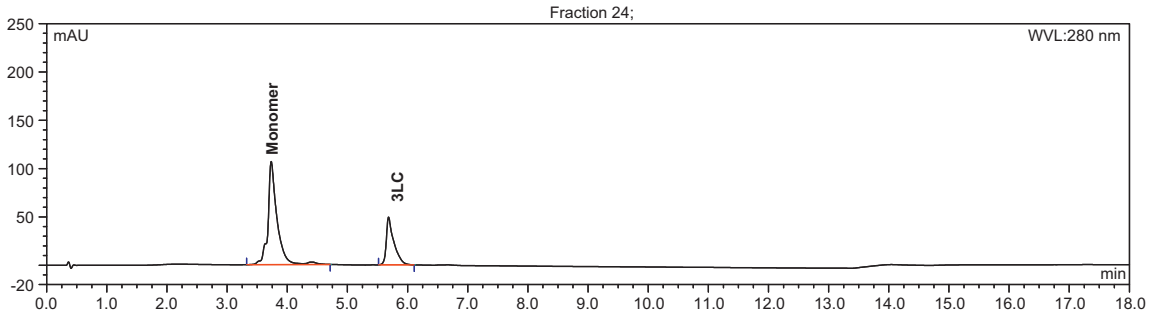

Fig. 1. mAb A HPLC-HIC chromatogram.

aggregate on cation exchange resins is significantly different, an indication that the mechanism which drives resolution of these two species is primarily electrostatic. However, a comparative study of SP Sepharose™ FF and SP Sepharose™ XL revealed that while the difference in characteristic charge (also known as the protein effective binding charge) between monomeric and aggregated forms of a recombinant monoclonal antibody was much larger on SP Sepharose™ XL, the separation performance of the two resins was similar [5]. This is consistent with the work of Wu and Walters [9] who concluded that retention is not perfectly correlated with characteristic charge and must be influenced by other factors. DePhillips and Lenhoff compared the retention of several model proteins on a range of commercial resins and concluded that ligand type (sulfopropyl versus carboxylate) and pore size were the primary determinants of protein retention in cation exchange chromatography [13]. Clearly there exists a complicated relationship between resin properties and resin performance; understanding the role of individual characteristics such as ligand density or pore geometry in actual separation processes can be difficult without the use of sophisticated modeling techniques or resin prototypes that vary in only one aspect of their design.

The objective of this work was to elucidate the effects of ligand density in cation exchange chromatography operations. This was accomplished using a series of prototype preparative resins differing only in ligand density. The resins were packed into columns with representative bed heights and experiments were run in bind-and-elute mode. Three monoclonal antibody feedstocks with relatively high levels of product-related impurities and host cell proteins were used in an attempt to identify changes in yield and impurity clearance caused by ligand density variation. In all cases, the resins were operated at intermediate load densities and also near capacity to obtain a meaningful assessment of resin performance at conditions relevant to large scale biochemical manufacturing processes.

2. Materials and methods

2.1. Resins and columns

Experiments were performed on five cation exchange (CIEX) resins provided by GE Healthcare Bio-Sciences (Uppsala, Sweden). These resins consisted of sulphopropyl (SP) ligands coupled to the same type of cross-linked agarose base matrix as that used in Capto™ ImpRes. Mean particle size was approximately 46 μm. Ligand densities were as follows: 0.045 eq/L (45 meq/L), 0.064 eq/L (64 meq/L), 0.103 eq/L (103 meq/L), 0.141 eq/L (141 meq/L), 0.154 eq/L (154 meq/L). This range of ligand densities extends far below the commercial specification of 0.13–0.16 eq/L for Capto™ SP ImpRes.

All resins were packed into 0.66 cm i.d. × 20 cm Omnifit columns (Bio-Chem Valve, Inc., Cambridge, England). All column chromatography experiments were performed on an ÄKTA™ Explorer 100 FPLC system (GE Healthcare, Piscataway, NJ) with a 2 mm pathlength UV cell.

2.2. Feedstock

Full-length monoclonal antibodies (mAbs) were expressed in Chinese hamster ovary (CHO) cells in 2000 l bioreactors at Genentech (South San Francisco or Oceanside, CA). Cell culture fluid was harvested using a combination of continuous centrifugation and depth filtration. Harvested cell culture fluid was initially purified using Protein A affinity chromatography with low pH elution in 0.10–0.15 M acetic acid. Protein A eluate was adjusted to pH 5.5 with 1.5 M Tris base and loaded onto the lab scale cation exchange columns without further adjustment.

Table 1 lists the antibodies used in this work. mAb A was engineered with an unpaired cysteine residue on each heavy chain. This resulted in a covalent "triple light chain" (3LC) high molecular weight variant which comprised approximately 10% of the cation exchange load by mass (see Section 2.3). mAb B cation exchange load was comprised of approximately 11% aggregate by mass; in this case, the high molecular weight species were primarily covalent dimers and trimers as verified by high performance size exclusion chromatography (see Section 2.4) and SDS-PAGE. mAb C had nearly undetectable levels of high molecular weight variants, but the cation exchange load had relatively high levels of host cell protein (HCP) impurities (approximately 10-fold higher than other mAbs employed in this study).

2.3. High performance hydrophobic interaction chromatography (HPLC-HIC)

An HPLC-HIC assay was used to quantify the amount of 3LC in the cation exchange load and eluate for mAb A. The assay used a TSKgel Butyl-NPR (4.6 mm × 35 mm) column (cat. No. 14947) from Tosoh Bioscience (Montgomeryville, PA). The column was run at 0.8 mL/min for 18 min. Buffer A was 1.5 M ammonium sulfate, 25 mM sodium phosphate, pH 6.95. Buffer B was 25 mM sodium phosphate, pH 6.95 with 25% isopropyl alcohol by volume. Protein was eluted with a gradient of 0–100% B in 12 min with UV

Table 1
Monoclonal antibody feedstock.

Property	mAb A	mAb B	mAb C
Framework	IgG1	IgG1	IgG1
Theoretical pI	9.4	8.9	8.5
pH of cation exchange load	5.5	5.5	5.5
Conductivity of cation exchange load (mS/cm)	4.3	4.0	4.1
HMW species in protein A pool (%)	10	11	<1
Approximate HCP in protein A pool (ng/mg[a])	2000	8000	40,000

[a] ng of HCP/mg antibody.

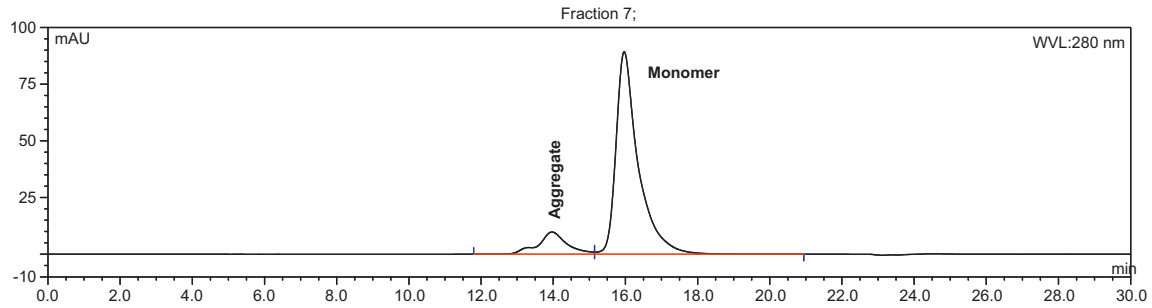

Fig. 2. mAb B HPLC-SEC chromatogram.

detection at 280 nm. Following gradient elution, the column was re-equilibrated in Buffer A for 6 min. The column was run at ambient temperature. The target mass for each injection was 50 μg. Fig. 1 shows a typical chromatogram for mAb A.

2.4. High performance size exclusion chromatography (HPLC-SEC)

An HPLC-SEC assay was used to quantify the amount of aggregate in the cation exchange load and eluate for mAb B. The assay used a TSK G3000SWXL (7.8 × 300 mm) column (cat. No. 08541) from Tosoh Bioscience (Montgomeryville, PA). The column was run at 0.5 mL/min for 30 min in 0.20 M potassium phosphate, 0.25 M potassium chloride, pH 6.2. The column was run at ambient temperature and monitored at 280 nm. The target mass for each injection was 50 μg. Fig. 2 shows a typical chromatogram for mAb B.

2.5. Dynamic binding capacity experiments

The resin dynamic binding capacities at 1% breakthrough ($DBC_{1\%}$) were measured at 150 cm/h (8 min residence time). For purposes of this study, 1% breakthrough was defined as the column load density (grams of antibody loaded per liter of packed bed) at which antibody concentration in the column effluent was equal to one percent of the antibody concentration in the load.

Column effluent was collected in 2 mL fractions, and the concentration of antibody in the fractions was quantified by UV absorbance at 279 nm.

2.6. Column chromatography – assessing HMW clearance

The cation exchange columns were initially equilibrated with five column volumes (CV) of 50 mM acetate, pH 5.5. mAbs (adjusted to approximately pH 5.5 and 4 mS/cm as described in Section 2.2) were then loaded on the column to a density of 10 mg of antibody per milliliter of column bed volume or 80% of $DBC_{1\%}$. The columns were washed with five CV of 50 mM acetate, pH 5.5. Antibody was eluted with a 10–90% gradient in 15 CV. Buffer A was 50 mM acetate, pH 5.5. Buffer B was 500 mM acetate, pH 5.5. Eluate was collected in 2 mL fractions.

Elution fractions were analyzed using HPLC-HIC for mAb A (see Section 2.3) or HPLC-SEC for mAb B (see Section 2.4). The percent of HMW impurity present in the cumulative end product pool (%HMW) was calculated as follows:

$$\%\mathrm{HMW} = \frac{\sum_{i=1}^{n}(C_i[\mathrm{mg/mL}])(\mathrm{HPLC}_i)}{\sum_{i=1}^{n}(C_i[\mathrm{mg/mL}])} \times 100 \quad (1)$$

where C_i is the mAb concentration in fraction i, HPLC_i is the mass fraction of HMW species present in fraction i, and n is the number of fractions collected at any point during elution. Collection of fractions was started at a UV absorbance of 0.5 OD (optical density) which corresponds to 100 mAu on the detector employed in this study. Fraction collection was stopped at 0.5 OD.

2.7. Column chromatography – assessing charge variant profile and HCP clearance

The cation exchange columns were initially equilibrated with five column volumes (CV) of 50 mM acetate, pH 5.5. mAb A, mAb B, or mAb C (adjusted to approximately pH 5.5 and 4 mS/cm as described in Section 2.2) was then loaded on the columns to a density of 15 mg of antibody per milliliter of column bed volume or 80% of $DBC_{1\%}$. The column was washed with five CV of 50 mM acetate, pH 5.5. Antibody was eluted with a 10–90% gradient in 15 CV. Buffer A was 50 mM acetate, pH 5.5. Buffer B was 500 mM acetate, pH 5.5 (mAb A and mAb B) or 350 mM acetate, pH 5.5 (mAb C). Eluate was fractionated according to optical density (OD) at the outlet of the column; fractions corresponding to 0.5–2.0 OD, 2.0–1.0 OD, and 1.0–0.5 OD were collected. The distribution of charge variants in the elution pools was determined by imaged capillary isoelectric focusing (icIEF). Samples were treated with carboxypeptidase B prior to analysis. HCP in the elution pools was quantified using an ELISA that was developed at Genentech in well plate format.

3. Results and discussion

Dynamic binding capacity of the five prototype resins varied from 49 g/L to 70 g/L for mAb A, from 43 g/L to 65 g/L for mAb B, and from 42 g/L to 61 g/L for mAb C (see Fig. 3). On all of the resins the capacity for mAb A was highest followed by mAb B and mAb C; this trend correlates well with the isoelectric points of the antibodies (Table 1). In general, the binding capacity for each mAb increased with ligand density, although the $DBC_{1\%}$ versus ligand density curves appear to have inflection points around 100 meq/L. It has been shown that dynamic binding capacity increases with

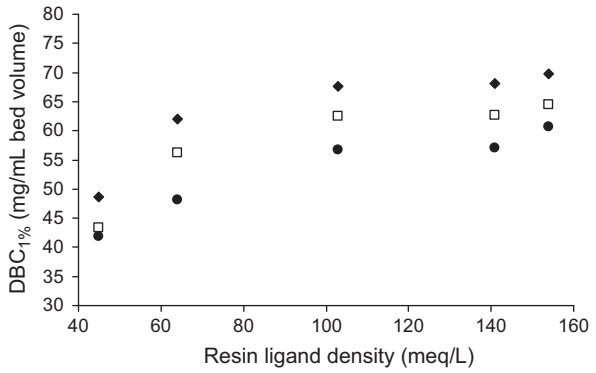

Fig. 3. mAb dynamic binding capacities at 1% breakthrough ($DBC_{1\%}$) on CIEX prototypes. (♦) mAb A, (□) mAb B, (●) mAb C.

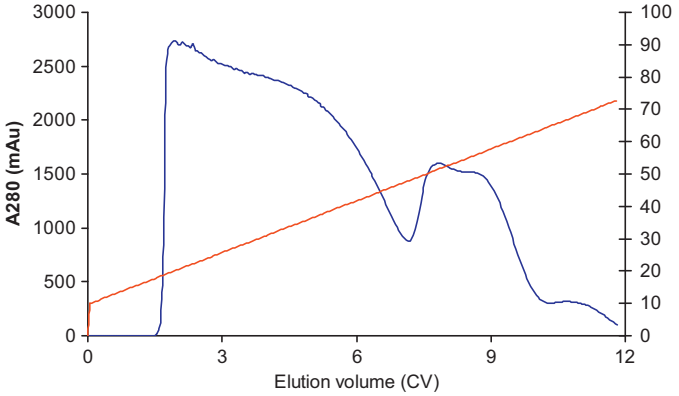

Fig. 4. mAb A on 154 meq/L CIEX prototype resin at 80% of $DBC_{1\%}$. The blue trace is UV absorbance at 280 nm and the red trace is % Buffer B. The *x*-axis has been normalized so that the start of gradient elution corresponds to 0 CV (column volumes). mAb concentration in the load material was 6.2 g/L; 62.5 mL Protein A pool loaded. (For interpretation of the references to color in this figure legend, the reader is referred to the web version of the article.)

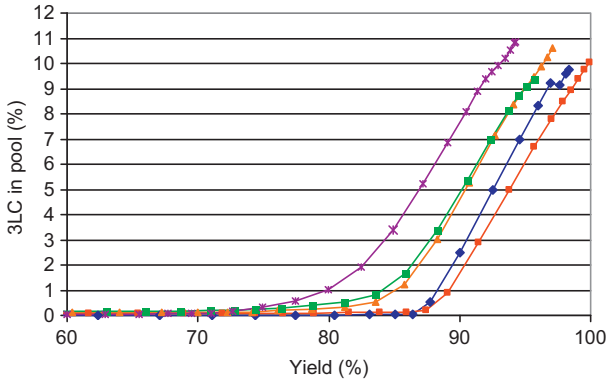

Fig. 5. 3LC versus total antibody yield for mAb A on CIEX prototypes at 80% of $DBC_{1\%}$. (♦) 45 meq/L, (■) 64 meq/L, (▲) 103 meq/L, (■) 141 meq/L, (X) 154 meq/L. Lines between the data points are for visual purposes only.

ligand density until a maximum characteristic charge is achieved [9]. However, Hardin and co-workers showed that dynamic binding capacity can be adversely affected by increasing ligand density due to steric exclusion effects at the resin surface [14]. The trends observed here may be a combination of these effects.

Resins with lower ligand density appeared to provide better clearance of HMW variants for mAb A. In this case the predominant HMW species was an approximately 175 kDa "triple light chain" (3LC) variant that was visibly resolved from monomer even

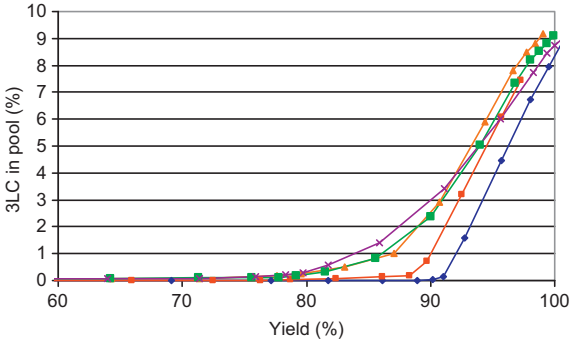

Fig. 6. 3LC versus total antibody yield for mAb A on CIEX prototypes at 10 g/L. (♦) 45 meq/L, (■) 64 meq/L, (▲) 103 meq/L, (■) 141 meq/L, (X) 154 meq/L. Lines between the data points are for visual purposes only.

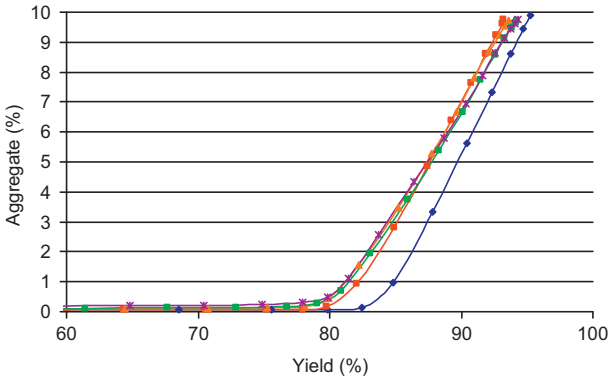

Fig. 7. Aggregate versus total antibody yield for mAb B on CIEX prototypes at 80% of $DBC_{1\%}$. (♦) 45 meq/L, (■) 64 meq/L, (▲) 103 meq/L, (■) 141 meq/L, (X) 154 meq/L. Lines between the data points are for visual purposes only.

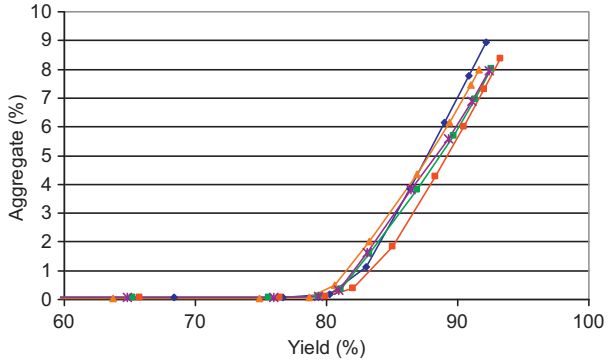

Fig. 8. Aggregate versus total antibody yield for mAb B on CIEX prototypes at 10 g/L. (♦) 45 meq/L, (■) 64 meq/L, (▲) 103 meq/L, (■) 141 meq/L, (X) 154 meq/L. Lines between the data points are for visual purposes only.

at very high loadings (see Fig. 4). When the resins were loaded to 80% of their respective $DBC_{1\%}$ values, the resin with ionic capacity of 154 meq/L clearly provided the least clearance of 3LC at any given yield (see Fig. 5). The resins with the second and third highest ionic capacities performed similarly and slightly better than the 154 meq/L resin. At the lowest ligand densities, there was a slight reversal in this trend; the resin with ligand density of 64 meq/L removed the most 3LC at any given yield, while the

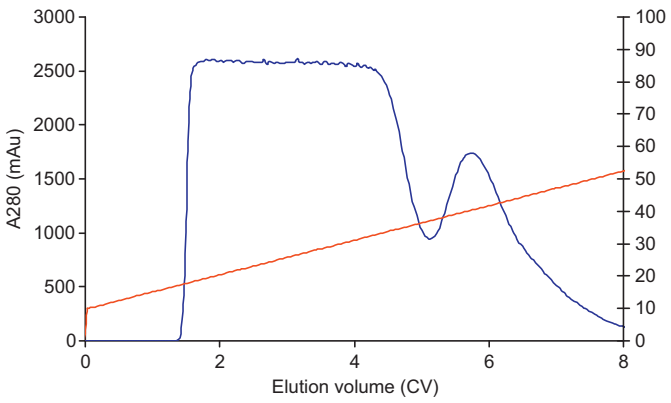

Fig. 9. mAb B on 154 meq/L CIEX prototype resin at 80% of $DBC_{1\%}$. The blue trace is UV absorbance at 280 nm and the red trace is % Buffer B. The *x*-axis has been normalized so that the start of gradient elution corresponds to 0 CV (column volumes). mAb concentration in the load material was 6.5 g/L; 57.6 mL Protein A pool loaded. (Note: the maximum absorbance read by the UV detector in these experiments is approximately 2500 mAu.). (For interpretation of the references to color in this figure legend, the reader is referred to the web version of the article.)

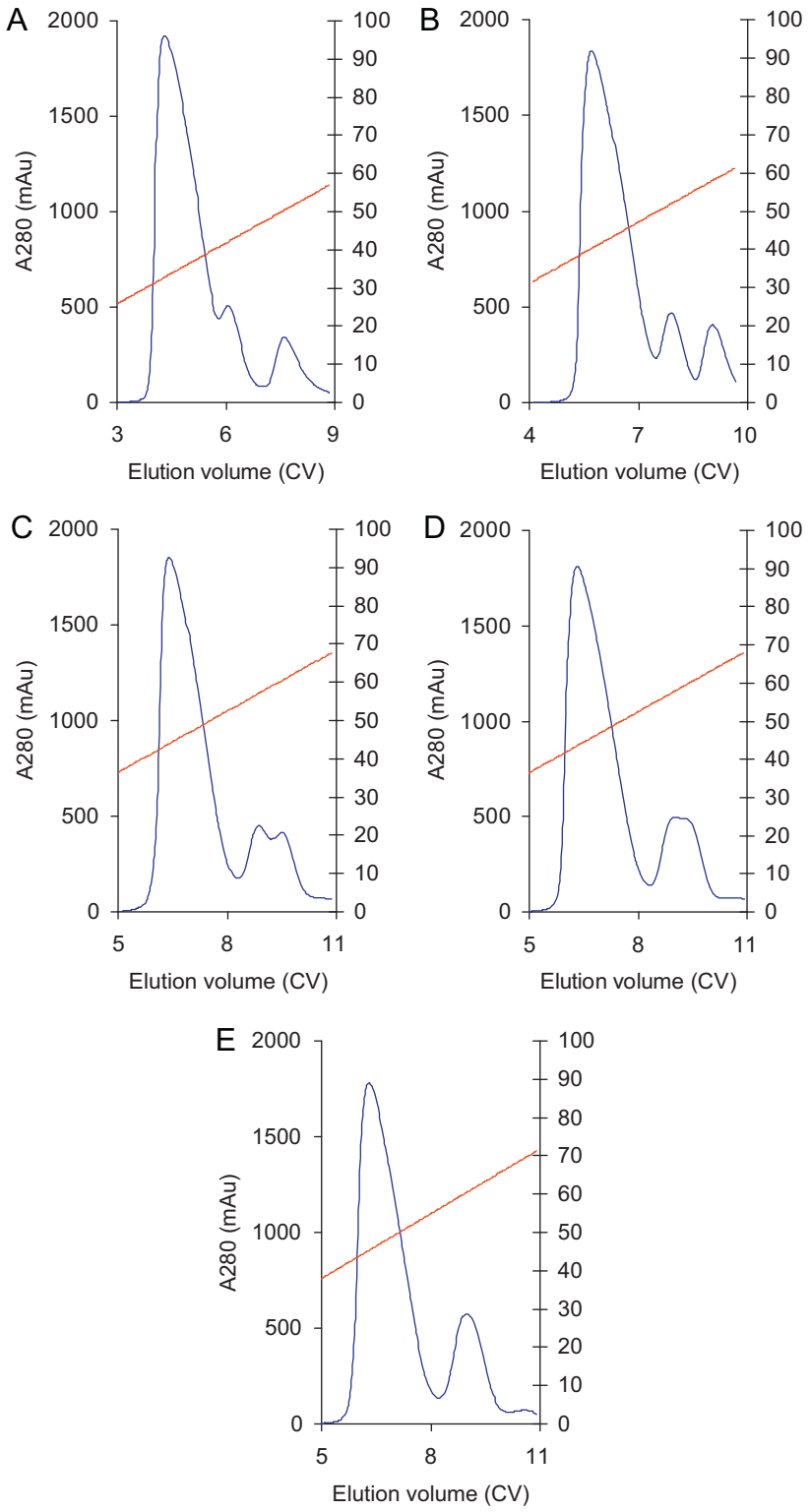

Fig. 10. mAb A on CIEX prototype resins at 10 g/L. (A) 45 meq/L, (B) 64 meq/L, (C) 103 meq/L, (D) 141 meq/L, (E) 154 meq/L. The blue trace is UV absorbance at 280 nm and the red trace is % Buffer B. The *x*-axis has been normalized so that the start of gradient elution corresponds to 0 CV (column volumes). (For interpretation of the references to color in this figure legend, the reader is referred to the web version of the article.)

lowest ligand density resin (45 meq/L) provided the second best clearance. Nonetheless, lower ligand density resins appeared to resolve monomer and 3LC better in this process. When all the resins were loaded to 10 g/L, the trend was similar – more 3LC variant was removed on the lower ligand density resins (see Fig. 6). In this case, the lowest ligand density resin did provide the best clearance, and the resin with second lowest ligand density removed slightly less 3LC at any given antibody yield. The performance of the three resins with highest ligand density was similar. This was a surprising result given the fact that Wu and Walters [9] reported *worse* resolution at lower ligand density for isocratic elution of two model proteins.

It is also interesting to note that protein load density affected the shape of the 3LC versus yield curves for mAb A. While lower ligand density resins appeared to provide better resolution of 3LC at both 80% of $DBC_{1\%}$ and 10 g/L, the total antibody yield seems to change with ligand density only when loading to 80% of $DBC_{1\%}$. (Here, the total antibody yield is the sum of the monomer and 3LC recovered from the column at the end of gradient elution and corresponds to the last data point on each curve. This data point represents a pool of all fractions collected during elution.) In Fig. 5, the total antibody yield was close to 100% for the 45 and 64 meq/L resins but decreased to 97% on the 103 meq/L resin, to 96% on the 141 meq/L resin, and to 94% on the 154 meq/L resin. In Fig. 6, all of the 3LC versus yield curves converge to approximately 100%. Since yield losses in preparative protein chromatography are often attributed to irreversible binding, it is not surprising that small decreases in yield were observed as ligand density increased. It may be that this effect was more pronounced at the higher adsorbed protein concentration because of aggregation or protein structural changes.

No trend in HMW clearance versus ligand density was observed for mAb B. At 80% of $DBC_{1\%}$, the lowest ligand density resin appeared to provide an advantage in aggregate clearance, but the other four resins all behaved similarly (see Fig. 7). At the lower protein load of 10 g/L, no clear trend was apparent among the resins (see Fig. 8). Further, protein load density had little to no effect on the shapes of these curves or the total antibody yields. Fig. 9 shows a typical chromatogram for mAb B.

Chromatograms for mAb A at 10 g/L protein load were compared in an attempt to elucidate the apparent contradiction in results from mAb A, mAb B, and the work of Wu and Walters (Fig. 10). From this, it became evident that retention differences of a third variant of mAb A were responsible for the trends observed when percent 3LC was plotted as a function of total antibody yield. The smaller, partially resolved peak in these chromatograms, identified by mass spectrometry as a basic charge variant, should elute after the monomer peak due to the presence of one additional positive charge imparted by a histidine residue at pH 5.5. (This variant was resolved best on the 64 meq/L resin and corresponds to the second peak in Fig. 10B.) Expression of basic charge variants occurs commonly in recombinant cell culture processes; these variants can be partially resolved on preparative ion exchange resins but are usually not completely removed [15]. Here, resolution of monomer and charge variant improves as resin ligand density increases, while resolution of charge variant and 3LC decreases. There is no obvious change in resolution of the main monomer and 3LC peaks as ligand density varies. Since charge variants co-elute with monomer on the HPLC-HIC assay used to analyze eluate fractions, resolution *appears* to decrease at higher ligand density when percent 3LC is plotted as a function of yield. In this situation lower ligand density resins would be desirable if the basic charge variants were to be pooled with the main product peak, but higher ligand density resins would be beneficial if the charge variant were considered an impurity.

Retention of monomeric, HMW, and charge variant species was compared by plotting the conductivity at maximum peak height as a function of resin ligand density. This data appears in Fig. 11 for the experiments at 10 g/L load density. For both mAb A and mAb B, the shape of the retention curve for monomer is similar to that for the HMW variant; the only significant difference between these curves is their relative positions on the plot. In other words, ligand density does affect the retention of both monomeric and HMW antibody species, but the retention of each variant is changed to a similar extent at every ligand density. Hence, the net change in resolution is negligible. The mAb A basic charge variant is the only instance in this study where changing ligand density changed retention of an impurity to a different extent than the monomer. While gradient slope does influence the conductivity at maximum peak height in a linear gradient elution [16] (and decreasing the gradient slope would likely improve resolution of monomeric and HMW species at all ligand densities), it is unlikely that incremental changes in the gradient slope would reveal an optimal ligand density that imparts better resolution of HMW species than others.

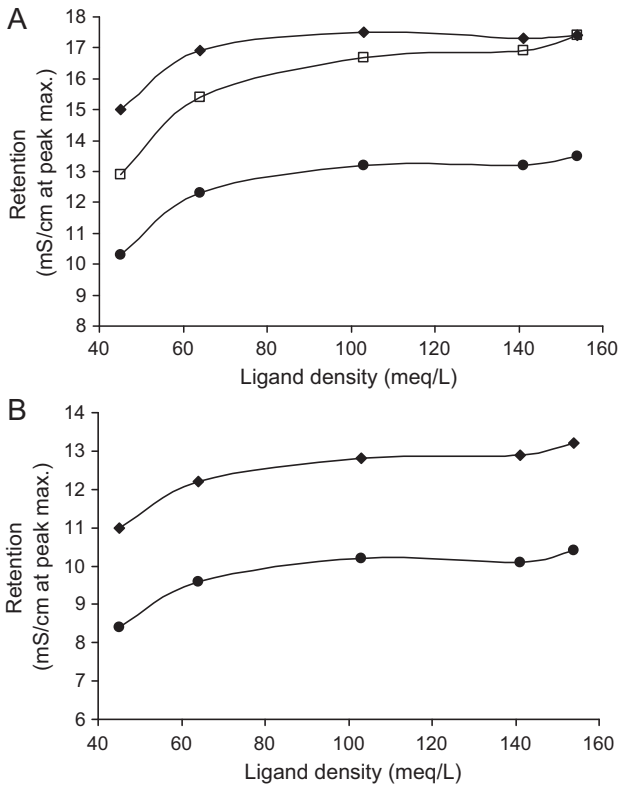

Fig. 11. Retention as a function of ligand density for gradient elution experiments at 10 g/L load density on CIEX prototypes. (A) mAb A: (●) monomer, (□) charge variant, (♦) triple light chain variant. (B) mAb B: (●) monomer, (♦) aggregate. Lines between the data points are for visual purposes only.

The mAb A data is partially consistent with results of molecular dynamics simulations performed by Dismer and Hubbuch [17] which indicated that selectivity is improved on surfaces with higher ligand density. In that work, the authors calculated the electrostatic energy for interaction of lysozyme with a two dimensional surface and found that energetic differences for various binding orientations of the protein grew larger as ligand spacing was reduced. This interpretation of selectivity is consistent with the behavior of mAb A monomer and charge variant, which presumably have different surface charge distributions and resolved better on the high ligand density resins. However, the retention difference of the charge variant and the HMW variant actually became smaller as ligand density increased (Fig. 11). Assuming that monomer and HMW species have similar surface charge distributions but different characteristic charges (Suda and co-workers have already confirmed the latter [5]) and that charge variants differ in both surface charge distribution and characteristic charge, one explanation for the observations in this study is that surface charge distribution strongly influences the shape of the retention versus ligand density curve, but characteristic charge only influences the position of the curve up or down. This would explain why resolution of monomer and HMW species did not change with ligand density and why the charge variant was better resolved from monomer but less resolved from the HMW variant at high ligand density. Regardless of the mechanism that truly controls this behavior, it seems that the shape of the retention versus ligand density curve and the relative position of protein

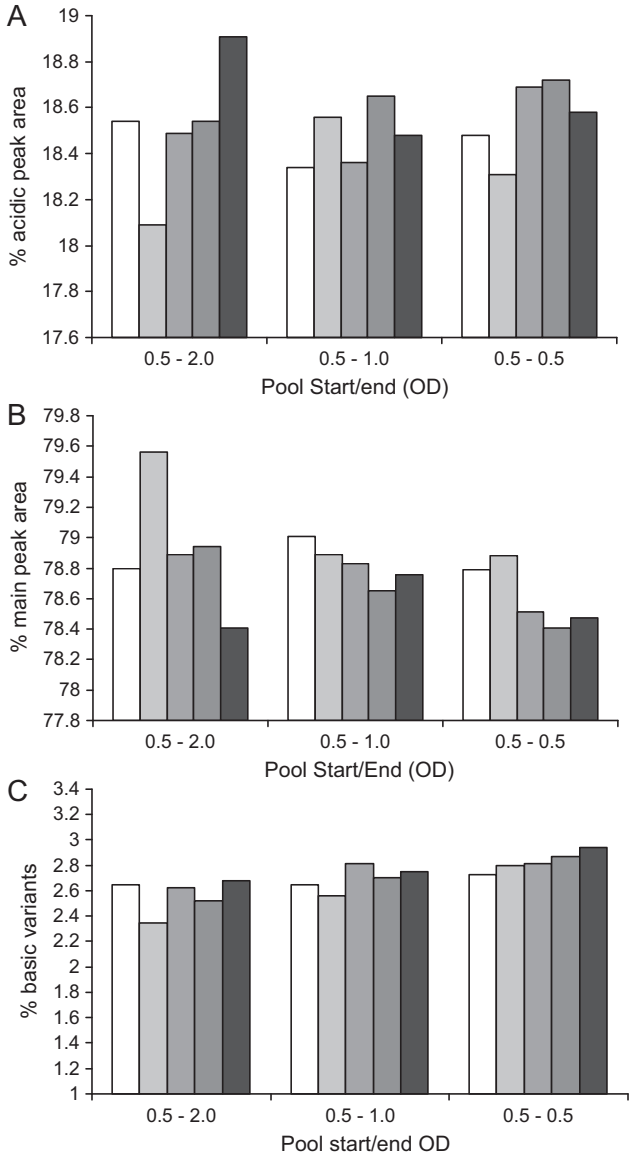

Fig. 12. Distribution of charge variants in cation exchange chromatography pools for mAb C loaded to 15 g/L on CIEX prototypes. (A) Acidic variants, (B) Main peak, (C) Basic variants. Resins: (□) 45 meq/L, (■) 64 meq/L, (■) 103 meq/L, (■) 141 meq/L, (■) 154 meq/L. NOTE: OD = optical density.

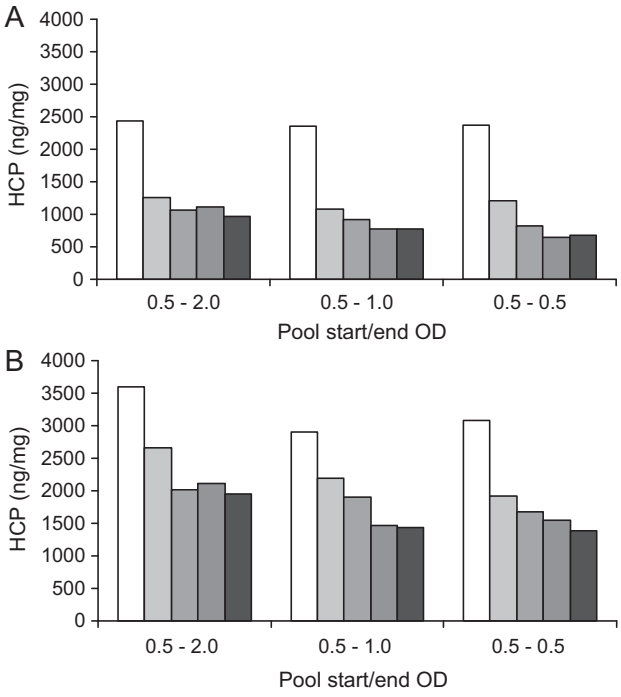

Fig. 13. Host cell protein levels in cation exchange chromatography pools for mAb C on CIEX prototypes. Yields were between 95 and 100% for all elution pools. (A) Loaded to 15 g/L, (B) Loaded to 80% of $DBC_{1\%}$. Resins: (□) 45 meq/L, (■) 64 meq/L, (■) 103 meq/L, (■) 141 meq/L, (■) 154 meq/L.

species on those curves will determine whether better resolution occurs at high or low ligand density.

While mAb A provides an interesting example for studying the connections between retention and resolution in preparative ion exchange chromatography, this case is not representative of most therapeutic antibody candidates which present a range of charge variants (including C-terminal lysine variants and deamidated species) all present at very low levels. To further explore the resolution of charge variants in cation exchange chromatography, a third antibody with a more typical distribution of charge variants and no HMW variants was introduced into the study. The charge variants of this antibody, mAb C, were not preferentially resolved on high or low ligand density resins (Fig. 12). With the possible exception of basic variants in the widest elution pool, there was no correlation between any of the icIEF peak areas and resin ligand density. Since basic charge variants would be expected to elute after acidic variants and main peak isoforms in cation exchange chromatography, extending the elution pool might elucidate any trends related to basic charge variants and ligand density; however, the differences in percent basics observed here are so small that they are inconsequential for practical purposes.

In contrast, a relationship between host cell protein (HCP) clearance and resin ligand density was observed for mAb C. In this case, impurity clearance improved as ligand density increased, up to approximately 100 meq/L (Fig. 13). The trend in HCP clearance was qualitatively similar to the trends in dynamic binding capacity and retention – changes occurred as ligand density increased, but only up to a point. This data is consistent with the predictions of Dismer and Hubbuch [17] in the sense that selectivity for the antibody was better at higher ligand densities; however, it is important to note that HCP (as reported in this study) represents a large collection of proteins with diverse biophysical characteristics. While the majority of HCP, as detected by the ELISA, were cleared more effectively on higher ligand density resins, it is entirely possible that there exists a subset of HCP which is better resolved on lower ligand density resins. Further, this relationship was not observed for mAb A or B; in these cases, HCP clearance was unchanged as ligand density was varied (data not shown). This may be explained by the fact that each antibody associates with a unique population of HCP and carries it forward from Protein A to downstream processing steps. Studies by Sisodiya and co-workers have shown that the concentration and distribution of HCP species in preparative Protein A pools is highly antibody-specific [18]. The level of HCP in the mAb C Protein A pool was approximately 10-fold higher than that for mAb A or mAb B. These results indicate that clearance of HCP can be affected by large changes in resin ligand density, although this effect will be highly dependent on feedstock.

4. Conclusions

Ligand density can affect selectivity in preparative cation exchange chromatography, but the nature and extent of this effect is highly dependent on feedstock. Based on results from this work, separation performance could improve, decline, or stay the same

as ligand density is increased. This was illustrated by a monoclonal antibody with three major variants: monomer, 3LC (175 kDa), and a basic charge variant. As ligand density increased, resolution of the monomer and charge variant improved, but resolution of charge variant and 3LC became worse. Resolution of monomer and 3LC did not change with ligand density. In this case, selection of the ideal ligand density from a process development perspective would hinge on whether or not the charge variant was considered an impurity. Experiments with a second antibody were consistent in the sense that no change in clearance of high molecular weight variants (in this case, covalent aggregates) was observed as ligand density increased. The relationship between ligand density and resolution is not straightforward and can be influenced by the biophysical characteristics of the individual protein species being processed; however, it appears that resolution of monomeric and high molecular weight antibody forms is insensitive to ligand density.

In this study, it appears that changes in separation performance were due to changes in retention rather than mass transfer effects such as those associated with steric hinderance at the surface of the resin beads [14]. This is evidenced by the fact that dynamic binding capacity increased across the entire ligand density range examined; $DBC_{1\%}$ would be expected to decrease if ligand density was affecting transport into the resin pores. Further, the observations made in this study regarding HMW variant and HCP clearance were similar at both low (10 or 15 g/L) and high (80% of $DBC_{1\%}$) protein load densities. These data suggest that, while resin ligand density could be customized to tune process performance in certain instances, more robust processes would result from using resins manufactured with ligand densities above the level at which intrinsic protein retention changes significantly but below the level where mass transport is hindered. For the prototype resins employed here, this range appears to be approximately 100–150 meq/L.

Acknowledgements

The authors would like to thank Annika Forss, Eggert Brekkan, and Gunnar Malmquist (all at GE Healthcare Bio-Sciences) for technical discussions and GE Healthcare Bio-Sciences (Björkgatan 30 SE-751 84 Uppsala, Sweden) for graciously providing samples of cation exchange prototype resins used in this study.

References

[1] A.A. Shukla, B. Hubbard, T. Tressel, S. Guhan, D. Low, J. Chromatogr. B 848 (2007) 28.
[2] G.S. Blank, G. Zapata, R. Fahrner, M. Milton, C. Yedinak, H. Knudsen, C. Schmelzer, Bioseparation 10 (2001) 65.
[3] N. Tugcu, D.J. Roush, K.E. Göklen, Biotechnol. Bioeng. 99 (2008) 599.
[4] J.X. Zhou, S. Dermawan, F. Solamo, G. Flynn, R. Stenson, T. Tressel, S. Guhan, J. Chromatogr. A 1175 (2007) 69.
[5] E.J. Suda, K.E. Thomas, T.M. Pabst, P. Mensah, N. Ramasubramanyan, M.E. Gustafson, A.K. Hunter, J. Chromatogr. A 1216 (2009) 5256.
[6] R.V. Cordoba-Rodriguez, Biopharm. Int. 21 (2008) 44.
[7] A. Staby, M.-B. Sand, R.G. Hansen, J.H. Jacobsen, L.A. Andersen, M. Gerstenberg, U.K. Bruus, I.H. Jensen, J. Chromatogr. A 1069 (2005) 65.
[8] A. Staby, J.H. Jacobsen, R.G. Hansen, U.K. Bruus, I.H. Jensen, J. Chromatogr. A 1118 (2006) 168.
[9] D. Wu, R.R. Walters, J. Chromatogr. 598 (1992) 7.
[10] J.F. Langford, X. Xu, Y. Yao, S.F. Maloney, A.M. Lenhoff, J. Chromatogr. A 1163 (2007) 190.
[11] A. Franke, N. Forrer, A. Butté, B. Cvijetić, M. Morbidelli, M. Jöhnck, M. Schulte, J. Chromatogr. A 1217 (2010) 2216.
[12] A.S. Rosenberg, AAPS J. 8 (2006) E501.
[13] P. DePhillips, A.M. Lenhoff, J. Chromatogr. A 933 (2001) 57.
[14] A.M. Hardin, C. Harinarayan, G. Malmquist, A. Axén, R. van Reis, J. Chromatogr. A 1216 (2009) 4366.
[15] R.J. Harris, J. Chromatogr. A 705 (1995) 129.
[16] S. Yamamoto, A. Kita, Food Bioprod. Process. 84 (2006) 72.
[17] F. Dismer, J. Hubbuch, J. Chromatogr. A 1217 (2010) 1343.
[18] V.N. Sisodiya, P.J. McDonald, K. Lazzareschi, M. Rodriguez, R. Fahrner, 1st International Conference on High-Throughput Process Development, Kraków, Poland, 2010.